Rev.Adv.Mater.Sci. 18(2008) 107-111

OXIDATION BEHAVIOUR OF A Cu-Zr-Al BULK METALLIC GLASS

C. Y. Tam[1], C. H. Shek[1] and W. H. Wang[2]

[1]Department of Physics and Materials Science, City University of Hong Kong, Tat Chee Avenue, Kowloon Tong, Hong Kong
[2]Institute of Physics, Chinese Academy of Science, Beijing, PR China

Received: March 29, 2008

Abstract. $Cu_{58.1}Zr_{35.9}Al_6$ bulk metallic glass (BMG) rod samples were prepared by suction casting into a water-cooled copper mould. The amorphous structure was confirmed with X-ray diffraction. The T_g and T_x were 760K and 799K, respectively, from differential scanning calorimetry (DSC) results. Thin disc samples were cut and oxidized at temperatures from 573K to 773K in an oxygen atmosphere inside a thermogravimetric analyzer. The oxidation kinetics can be described with a parabolic rate law from 673K to 753K but follows a linear rate law at 573K to 653K and 773K. The oxidation products are mainly Cu_2O, CuO and tetragonal ZrO_2 based on X-ray diffraction and grazing incidence XRD (GIXRD) results. However, a very thin layer of Al_2O_3, with thickness of only tens of nanometers, on the top surface of the oxide layer was revealed by Auger electron spectroscopy (AES) depth profiles. This aluminium oxide layer is thought to contribute to the exceptionally good oxidation resistance at elevated temperatures compared with that of $Cu_{60}Zr_{30}Ti_{10}$ we reported previously.

1. INTRODUCTION

In the last decade, lots of efforts were devoted to the development and investigation of Zr based metallic glasses due to their excellent glass forming ability. Recently, researchers pay particular attention to the Cu based bulk metallic glasses (BMG) owing to their superior mechanical properties [1,2], and the possibility of casting them into bulk form even with a binary copper alloy [3]. The prospect of developing Cu based BMG with very good glass forming ability is therefore promising.

In order for a Cu based BMG to be a practical structural material, the issue of the resistance to environmental attacks such as corrosion and oxidation must be carefully addressed in addition to the mechanical performance. Large number of works were done on the oxidation of metallic glass ribbons [4-11] but only a few can be found on BMGs [12-14]. Kimura *et al.* [15] reported that ZrO_2, copper oxides and metallic copper formed after oxidation of Cu-Zr metallic glass ribbon. Besides, pervious studies [16,17] revealed that Cu segregation phenomenon occurred during surface oxidation of Cu-Zr metallic glass. Investigation of the surface properties such as corrosion [18-21], nanoindentation [22], and nanoscratch [23] have been done in Cu based BMGs. However, few literatures [24] can be found in the oxidation behavior of Cu based bulk metallic glasses. The purpose of this present paper is to examine the oxidation behavior of a Cu based bulk metallic glass with good glass forming ability and the effects of aluminium on the resistance to oxidation.

Corresponding author: C. H. Shek, e-mail: apchshek@cityu.edu.hk

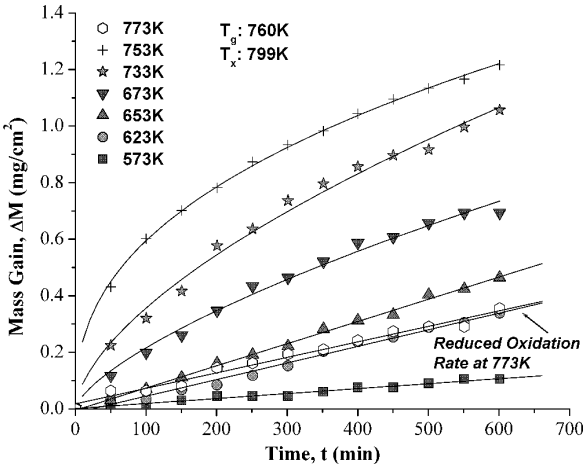

Fig.1. Oxidation kinetic of $Cu_{58.1}Zr_{35.9}Al_6$ metallic glass.

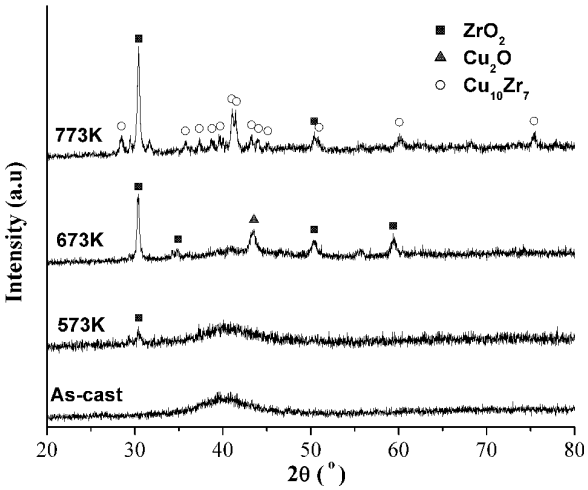

Fig. 2. XRD pattern of as-cast and oxidized $Cu_{58.1}Zr_{35.9}Al_6$ metallic glasses.

2. EXPERIMENTAL PROCEDURE

$Cu_{58.1}Zr_{35.9}Al_6$ (denoted as CZA hereafter) bulk metallic glass sample with 3mm diameters were prepared by arc melting the mixtures of Cu, Zr, and Al metals with purities better than 99.9 wt.% in a Ti-gettered argon atmosphere followed by suction casting into a copper mold. The T_g and T_x of the BMG are 760K and 799K, respectively, as measured in a purified nitrogen atmosphere with a Perkin Elmer DSC 7 using a constant heating rate of 20 K/min. The oxidation treatment and subsequent characterizations of the samples were performed with procedure and equipment similar to those described in our previous papers [25] for comparison of the effect of substituting aluminium for titanium.

The amorphous structure and oxide phases were identified with a Siemens D500 diffractometer using CuK_α (λ=0.15406 nm) radiation. Samples of around 2 mm thick for oxidation experiments were cut from the 3 mm diameter sample rods. The disc samples were ground with SiC paper and then polished with 5 micron aluminium oxide powder to mirror surface before performing the oxidation test. The mass gain during oxidation was measured by a Seiko Instrument TG/DTA 220 in oxygen environment with a constant flow rate of 500 mL/min. The samples were heated at a heating rate of 20 K/min from room temperature to the selected temperatures between 573K and 773K at which the samples were held isothermally for 10 hours. Grazing incidence X-ray diffraction (GIXRD) of the oxidized samples was carried out using CuK_α radiation on a Bruker AXS D8 Discover X-ray diffractometer with parallel beam optics. AES measurements of the oxide layer were done with an ULVAC-PHI 5802 system equipped with a LaB_6 filament and the electron beam energy set at 10 keV. Depth profiles were obtained using Ar^+ sputtering at 4 keV. The oxide morphologies were examined with a JEOL JSM-820 scanning microscope operating at 20 kV.

3. RESULTS AND DISCUSSIONS

The variations of mass gains of the CZA BMG with oxidation time at different temperatures are shown in Fig. 1. In general, the oxidation rate increases with temperature up to 753K, and then drops significantly at 773K. The drop in oxidation rate at 773K, which is close to T_x, may result from the formation of the stable intermetallic crystalline phase as shown in Fig. 2. Besides, it can be seen that the metallic glass has two distinct types of oxidation kinetics at different temperature ranges. It exhibits linear behavior when oxidized at 573K to 653K while a parabolic rate law is obeyed at 673K to 753K. At 773K, it reverts to the linear rate law again and the oxidation kinetics is similar to that of the sample oxidized at 623K. When oxidized at low temperatures, only surface reaction between the adsorbed oxygen and the atoms on the metallic glass surface occurs and results in linear oxidation. However, during high temperature oxidation, the pro-

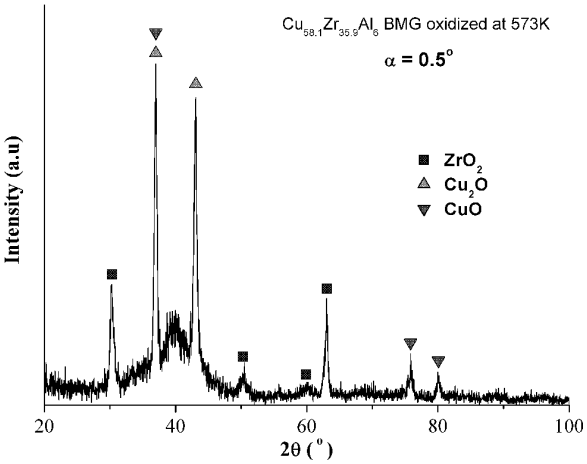

Fig. 3. GIXRD curve of $Cu_{58.1}Zr_{35.9}Al_6$ metallic glass oxidized at 573K.

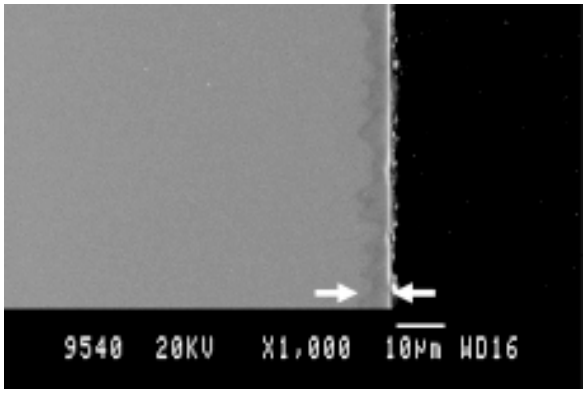

Fig. 4. Cross-sections of $Cu_{58.1}Zr_{35.9}Al_6$ BMGs oxidized at 673K. The thickness of the oxide layers are indicated with the arrows.

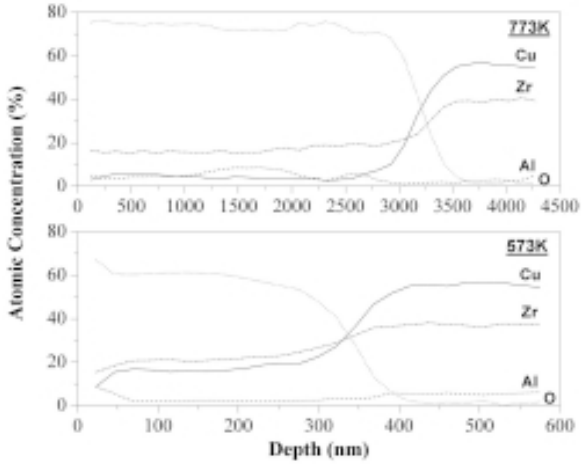

Fig. 5. AES depth profiles of CZA oxidized at 773K and 573K.

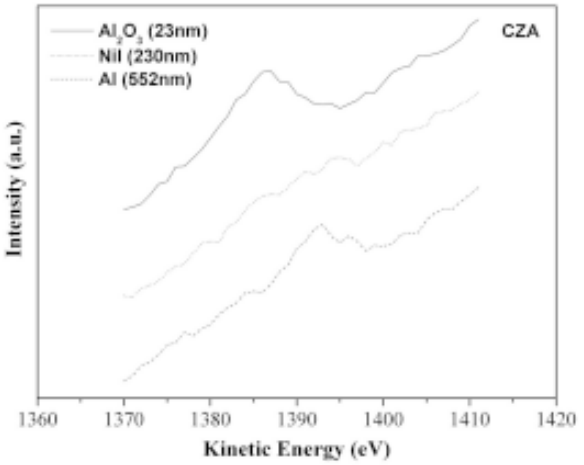

Fig. 6. AES spectrum of Al in CZA oxidized at 573K.

cess is controlled by the diffusion of ions through the oxide layer. The process can be either by the diffusion of the metal ions through oxide layer to the adsorbed oxygen ions on the metallic glass surface or the diffusion of the oxygen anions through the oxide to the metallic glass. The types of elements dominating the oxidation process of the metallic glass determine the direction of ionic diffusion in the oxide layer. For the Cu based metallic glass used in this investigation, the oxidation process is thought to proceed by inwards diffusion of oxygen reacting with Zr to form ZrO_2 [25].

Fig. 2 displays the XRD pattern of as-cast and oxidized metallic glasses. The XRD pattern of the sample oxidized at 573K is similar with that of the as-cast sample, showing an amorphous peak, but with an additional ZrO_2 peak. In the sample oxidized at 673K, the oxide phases become dominant and they are identified as ZrO_2 and Cu_2O. The sample crystallized at 773K and the crystalline phase is mainly found to be $Cu_{10}Zr_7$ which is consistent with the previous report [26].

The sample oxidized at 573K was also examined with GIXRD, results as shown in Fig. 3, for a detailed study of the structure of the surface oxide film. The angle of incidence (a) of the X-rays was kept at 0.5°. The penetration depth of X-ray in ZrO_2 and copper oxides are estimated with Eq. (1) to be around 0.4 μm and 0.9 μm, respectively.

$$G(x) = 1 - e^{-\mu x\left[\frac{1}{\sin(\alpha)} + \frac{1}{\sin(2\theta-\alpha)}\right]}, \quad (1)$$

where x is the effective depth of penetration and μ is the linear absorption coefficient .

In addition to the amorphous diffuse peak and ZrO_2 peak as shown in Fig. 2, two more oxide phases, namely, Cu_2O and CuO are found. The grain sizes of the ZrO_2 and copper oxides were estimated with the Scherrer formula, $d = \lambda/\Delta \cdot \cos\theta_B$ [27] to be around 25 nm and 21 nm, respectively.

Fig. 4 displays the cross section of the oxide formed at 673K. The oxide thickness is around 3-6 mm. Comparing with our previous results for $Cu_{60}Zr_{30}Ti_{10}$ BMG [25], the oxide thickness and the rate of oxidation of the CZA BMG used in this study are only about one-third and one-third to one-sixth, respectively, of those for $Cu_{60}Zr_{30}Ti_{10}$ BMG. This difference may be explained in terms of the surface analysis results in the following.

Fig. 5 presents the Auger electron spectroscopy (AES) depth profiles of CZA oxidized at 573K and 773K. In both cases, the concentration of oxygen maintains at high level on the surface layer while those of other elements remain relatively low. The oxygen penetration depths, where the oxygen content drop rather abruptly to zero and the amount of the others return to the bulk level, of samples oxidized at 573K and 773K are found to be 400 nm and 3500 nm, respectively. Although no aluminium oxide is detected in XRD and GIXRD curves, the presence of Al_2O_3 in the oxidized CZA samples is apparent as shown in the AES spectrum in Fig. 6. The kinetic energy of Al (KLL) spectrum in the first 70 nm oxide layer is found to be 1387 eV, as shown in the 23-nm curve in Fig. 6, which shows good agreement with the oxide state of aluminium reported in previous finding [28]. The formation of Al_2O_3 can be attributed to its high negative heat of formation [29] compared with the oxides of Cu and Zr. However, owing to the low aluminium content in the alloy, only a very thin oxide layer can form. The Al_2O_3 at the topmost layer in CZA is a dense and stable oxide film that can protect the sample against further oxidation [30]. On the contrary, the copper oxides formed on $Cu_{60}Zr_{30}Ti_{10}$ BMG are not protective [25].

The heats of formation of CuO, Cu_2O, ZrO_2, and Al_2O_3 at 600K are -308.02, -339.90, -1094.97, and -1116.9 kJ/mol O_2, respectively [29]. Although formation of Al_2O_3 should be the most thermodynamically favorable, composition effect may dictate the reaction path in this case. The formation of ZrO_2 as the major oxidation product, as shown in Figs. 2 and 3, can be explained by the preferential oxidation owing to its high negative heat of formation as well as the high content. Kimura *et al.* [15] reported that only ZrO_2 was observed in oxidized $Zr_{70}Cu_{30}$ metallic glass but ZrO_2, Cu_2O and Cu were found in both $Zr_{50}Cu_{50}$ and $Zr_{37}Cu_{63}$. It is thought that the relatively low Al content in the Cu-Zr-Al metallic glass used in this investigation rendered the formation Al_2O_3 rather limited.

4. CONCLUSIONS

$Cu_{58.1}Zr_{35.9}Al_6$ bulk metallic glass exhibits good oxidation resistance in oxygen atmosphere even at temperatures close to its crystallization temperature. The oxidation kinetics follows a linear rate law at temperatures 573K to 653K and at 773K, while parabolic rate law was observed for temperatures 673K to 753K. In general, the oxidation rate increases with increasing oxidation temperature but decreases drastically at 773K, possibly due to the formation of the stable $Cu_{10}Zr_7$ intermetallic crystalline phase. The major oxide phases on the surface of the sample oxidized at 573K are ZrO_2, Cu_2O, and CuO. A very thin layer of Al_2O_3 with thickness in the order of tens of nanometers was revealed by the Auger electron spectra of the topmost layer of the oxidized surface. The surface layers of the sample oxidized at 773K consist mainly of ZrO_2 and a $Cu_{10}Zr_7$ crystalline phase.

ACKNOWLEDGEMENTS

This work was supported by a City University of Hong Kong Strategic Research Grant. (Project number: 7001991).

References

[1] A. Inoue, W. Zhang, T. Zhang and K. Kuroaska // *Acta Mater.* **49** (2001) 2645.
[2] A. Inoue, W. Zhang, T. Zhang and K. Kuroaska // *J. Non-Cryst. Solids* **304** (2002) 200.
[3] D. Xu, B. Lohwongwatana, G. Duan, W. L. Johnson and C. Garland // *Acta Mater.* **52** (2004) 2621.
[4] A. Dhawan, K. Raetzke, F. Faupel and S. K. Sharma // *Phys. Status Solidi A* **199** (2003) 431.
[5] L. Jastrow, U. Köster and M. Meuris // *Mater. Sci. Eng. A*, in press.
[6] M. C. Kim and M. J. McNallan // *Mater. Sci. Eng. A* **134** (1991) 1078.
[7] G. Wei and B. Cantor // *Acta Metall.* **36** (1988) 2293.
[8] A. M. Dark, G. Wei and B. Cantor // *Mater. Sci. Eng.* **99** (1988) 533.

[9] G. Wei and B. Cantor // *Acta Metall.* **36** (1988) 167.
[10] U. Köster, D. Zander, Triwikantoro, A. Rüdiger and L. Jastrow // *Scr. Mater.* **44** (2001) 1649.
[11] K. Mondal, U. K. Chatterjee and B. S. Murty // *J. Non-Cryst. Solids* **344-355** (2004) 544.
[12] M. Kiene, T. Strunskus, G. Hasse and F. Faupel, In: *Oxide Formation on the Bulk Metallic Glass* $Zr_{46.75}Ti_{8.25}Cu_{7.5}Ni_{10}Be_{27.5}$, ed. by W. L. Johnson, A. Inuoe and C. T. Liu (Mater. Res. Soc. Symp. Proc. 554, Warrendale, PA, 1999).
[13] S. K. Sharma, T. Strunskus, H. Ladebuschand F. Faupel // *Mater. Sci. Eng. A* **304-306** (2001) 747.
[14] W. Kai, H. H. Hsieh, T. G. Nieh and Y. Kawamura // *Intermetallics* **10** (2002) 1265.
[15] H. M. Kimura, K. Asami, A. Inoue and T. Masumoto // *Corrosion Sci.* **35** (1993) 909.
[16] M. Kilo, M. Hund, G. Sauer, A. Baiker and A. Wokaun // *J. Alloy. Compd.* **236** (1996) 137.
[17] A. Kudelski, M. Janik-Czachor, J. Bukowska, M. Pisarek and A. Szummer // *Mater. Sci. Eng. A* **326** (2002) 364.
[18] T. Yamamoto, C. L. Qin, T. Zhang, K. Asami and A. Inoue // *Mater. Trans.* **44** (2003) 1147.
[19] C. L. Qin, K. Asami, T. Zhang, W. Zhang and A. Inoue // *Mater. Trans.* **44** (2003) 1042.
[20] C. L. Qin, K. Asami, T. Zhang, W. Zhang and A. Inoue // *Mater. Trans.* **44** (2003) 749.
[21] K. Asami, C.-L. Qin, T. Zhang and A. Inoue // *Mater. Sci. Eng. A* **375-377** (2004) 235.
[22] C. A. Schuh and T. G. Nieh // *J. Mater. Res.* **19** (2004) 46.
[23] A. M. Hodge and T. G. Nieh // *Intermetallics* **12** (2004) 741.
[24] U. Köster, L. Jastrow and M. Meuris, *The 12th International Conference on Rapidly Quenched and Metastable Materials* (Jeju, Korea, 21-26 August 2005); Hoon Cho, Hanshin Choi, Hyungho Jo and Changhee Lee, ibid.
[25] C. Y. Tam and C. H. Shek // *J Mater. Res.* **20** (2005) 1396; *J Mater. Res.* **20** (2005) 2647.
[26] W. Zhang and A. Inoue // *Mater. Trans*. **44** (2003) 2220.
[27] B. D. Cullity, *Elements of X-ray diffraction, second ed*. (Addison-Wesley, Reading, 1978).
[28] E. Wieser, H. Reuther and E. Richter // *Nucl. Instrum. Meth. B* **111** (1996) 271.
[29] I. Barin, *Thermochemical Data of Pure Substances* (VCH, Weinheim, 1993).
[30] Gabriel Plascencia, Torstein Utigard and Tanai Marín // *JOM*, January (2005) 80.